Resonant Reflectance Anomalies: Effect of Shapes of Surface Irregularities

D. W. Berreman

Bell Telephone Laboratories, Murray Hill, New Jersey 07974

(Received 27 May 1969; revised manuscript received 9 October 1969)

It was recently shown that hemispherical pits or bumps on an otherwise flat surface of a sample of isotropic material may cause marked anomalies in reflectance near resonant frequencies of the material, such as reststrahlen bands in ionic dielectrics and plasma frequencies in metals. The anomalies occur even when such irregularities are much smaller than the wavelength of the reflected radiation, so that incoherently scattered radiation is negligible. The effect is due to localized resonances that are somewhat displaced in frequency from the bulk optic modes of the material by electric boundary conditions. The sharp right angle at the rim of a hemispherical pit or bump might have been suspected of giving exceptional results. In this paper, the problem is solved in a different way to demonstrate that pits and bumps with well-rounded edges produce anomalies of approximately the same magnitude and frequency characteristics as hemispherical pits and bumps. The effect is derived classically. Spatial dispersion and dielectric nonlinearity are assumed to be negligible. The effects of very slight roughness on the reflectance curves of lithium fluoride and of aluminum are described as illustrations.

I. INTRODUCTION

IN two recent papers,[1,2] the author described the effect that surface roughness in the form of minute hemispherical pits or domes well separated from one another would have on reflection near reststrahlen bands, plasmon frequencies, or other optical-resonance frequencies in isotropic media. The effect is due to electrically polar resonances in the material in the neighborhood of such pits or bumps. The resonances are displaced in frequency from the bulk optic-mode frequencies of the material because of electric fields induced around the curved surfaces of the bumps or pits. It is a coherent effect that causes changes in reflectance even when incoherent scattering is negligible. In the earlier papers we assumed negligible spatial dispersion or similar effects[3] and used classical electromagnetic theory and a spherical harmonic expansion. Later, we found, upon computing the electric polarization strength as a function of position around such bumps and pits, that the polarization was strongest in the immediate vicinity of the sharp rim of the hemispheres when the dielectric constant was such that the pits or bumps caused a large perturbation on the reflectance of the medium. This fact suggested the possibility that the magnitude of the effect might be exaggerated in hemispheres because of the sharp angle at the rim of such a bump or pit. Consequently, we have again solved the problem in a different way that allows us to find results for minute bumps or pits of any form that is a figure of revolution about an axis

normal to the generally flat surface of the medium. We checked the new method by using it for isolated spherical particles and obtained results very near to those that can be obtained analytically. We also reconfirmed the results we reported earlier for radiation incident normally on a surface with hemispherical pits and bumps except for a simple error factor that is described in Ref. 2. In addition, we have computed the effect on reflectance of normally incident radiation caused by minute pits or bumps with well-rounded edges. We find that the magnitude and frequency dependence of the effect for irregularities of fixed volume are not changed much if the edges of the pits or bumps are rounded, unless they are quite shallow and broad.

A general first-order approximation to the reflectance of a surface with small, isolated pits or bumps has been[2] (and will again be) shown to be of the general form

$$\mathcal{R} = \mathcal{R}_0 + N V \delta / \lambda, \qquad (1)$$

subject to the restrictions mentioned at the beginning and in the third section. In this expression, $\mathcal{R}_0$ is the reflectance of a perfectly smooth surface, N is the number of pits or bumps per unit area distributed randomly over the surface, V is the volume of an average pit or bump, λ is the wavelength of the reflected radiation, and δ is a form factor that depends on dielectric constant or refractive index, on the shape of the pit or bump, and on the angle of incidence of the radiation but not on the volume of the bump or pit as long as its dimensions are small compared to the wavelength of radiation involved. In the previous papers,[1,2] δ was shown to be roughly the same size for hemispherical bumps as for pits. (Errors in Refs. 1 and 2 described in Ref. 2 do not alter that conclusion.) In this paper, δ is shown also to be about the same size for pits or bumps with rounded contours as for hemispherical ones.

In these calculations, we have assumed that individual pits or bumps are isolated from one another

[1] D. W. Berreman, Phys. Rev. **163**, 855 (1967).

[2] D. W. Berreman, *Localized Excitations in Solids*, edited by R. F. Wallis (Plenum Press, Inc., New York, 1968), p. 420 ff. In both this and Ref. 1 there was an accumulation of errors so that the quantity whose imaginary part is equivalent to δ should have been multiplied by a factor $-(\epsilon+1)/(\sqrt{\epsilon}+1)$.

[3] See, e.g., J. J. Hopfield and D. G. Thomas, Phys. Rev. **132**, 563 (1963). Spatial dispersion is a name alluding to optical effects that occur when the ratio ϵ of electric displacement to electric field is nonlocal, and hence depends on proximity to surfaces. Hopfield and Thomas were interested in semiconductors. The anomalous skin effect in metals is also a nonlocal dielectric effect.

sufficiently that the field in the neighboring of one irregularity is not perturbed appreciably by neighboring imperfections. Although this assumption is invalid for many slightly rough surfaces, the fact that results are not strongly dependent on the shape of an individual irregularity may be used to argue that the results are not critically dependent on that assumption, as follows. A cluster of close bumps or pits (or, for simplicity, concentric rings) can be treated as a single imperfection. Such a treatment takes into account the interactions within the cluster more or less exactly. Since the resulting effect depends mostly on the total volume within the cluster and not so much on the details of its shape, we may conclude that the original assumption of sparse distribution is not essential to obtain the right order of magnitude of the effect.

Although solutions for obliquely incident radiation were found by a modification of the method to be described, the results are complicated and show nothing particularly different in reflectance. For simplicity, we will only treat the case of normally incident radiation in detail. The solution for oblique incidence is of interest in polarimetry, which is the subject of another paper to be published in the Journal of the Optical Society of America.

II. RELATION TO OTHER WORK

A large number of people have studied the subject of electromagnetic scattering by rough surfaces theoretically and experimentally. We will not attempt a complete resume of that work.[4] Much of the previous work was concerned with irregularities of sizes comparable to the wavelength of the incident radiation, as in gratings, and hence is not directly related to ours. Others have studied scattering by very small irregularities, but not in the neighborhood of resonances.[5] Much of such work has been based on the assumption that the medium is totally reflecting. In such calculations, losses from the coherent beam appear as incoherently scattered radiation. By contrast, the effect we are investigating is not an incoherent scattering effect. Another type of work that is also outside the realm of our investigation is that involving peculiarities in optical properties caused by abnormalities in the material itself very near its surface as in the anomalous skin effect, or to a nonlocal dielectric-dispersion relation (spatial dispersion).[3]

Strachan[6] investigated the effect of a monolayer of polarizable particles on a surface using Sommerfeld's rigorous theory of radiation by dipoles near a surface.[7] His results are useful in confirming the correctness of Eq. (6) below, which is derived heuristically.

The new or unusual features of the present work are the following. We have found more or less exact solutions, near resonant frequencies, to the boundary equations around very small bumps or pits of specific shapes that probably resemble many naturally occurring irregularities in fairly smooth surfaces. Enough different cases are treated to show how much (or little) importance to attach to the specific shapes of such irregularities. The computed anomalies in the reflectance may be surprisingly large. The technique used is perhaps somewhat unusual and is interesting not only for the present application but also because it can readily be adapted to solve many small-particle scattering problems that do not lend themselves to analytic solution.

Recent work on resonant electromagnetic scattering by rough surfaces or small particles is described in Refs. 1, 2, and 8–13.

III. METHOD OF SOLUTION

We assume that each pit is small enough compared to the wavelength of the incident radiation that we may make a quasistatic approximation to compute electric fields in the immediate neighborhood of each pit. That is, we may say that at a moderate distance from a pit, the electric field is approximately uniform and that fields near the pit are approximately those that would result from application of a uniform, static far field, with the exception that the dielectric constant ϵ is to have the complex value characteristic of the frequency of the radiation rather than the "static" value. We also assume that the pits are far enough apart that field perturbations by one pit are negligible at any neighboring pit. In addition, we assume negligible spatial dispersion and a linear, scalar relation between electric displacement $\mathbf{D}$ and electric field $\mathbf{E}$. That is, $\mathbf{D} = \epsilon\mathbf{E}$, where ϵ is a scalar dielectric constant of the medium. We ignore any fixed charges that may be around. Then both $\mathbf{D}$ and $\mathbf{E}$ obey Laplace's equation everywhere except on the surface of the medium, where there is a surface divergence of $\mathbf{E}$. (The surface divergence, $\sigma = \mathrm{div}\mathbf{E}$, may be thought of as arising from induced surface charges, which are the ends of the dipoles induced by polarization of the medium.[14] These are "bound charges," of course, not free-surface charges brought in from some distant point.)

We use the symmetry of the pits, which are taken to be figures of revolution, to make the following

[4] An extensive review of older work can be found in P. Beckman and A. Spizzicheno, *The Scattering of Electromagnetic Waves from Rough Surfaces* (Pergamon Press, Inc., New York, 1963).
[5] H. E. Bennett and J. O. Porteus, J. Opt. Soc. Am. **51**, 125 (1961).
[6] C. Strachan, Proc. Cambridge Phil. Soc. **29**, 116 (1933).
[7] A. Sommerfeld, Ann. Physik **81**, 1135 (1926).

[8] Ye-Yung Teng and Edward A. Stern, Phys. Rev. Letters **19**, 511 (1967).
[9] O. Hunderi and D. Beaglehole, Phys. Letters **29A**, 335 (1969).
[10] H. Ehrenreich, H. R. Philipp, and B. Segall, Phys. Rev. **132**, 1918 (1963). [Data fitted with an oscillator model by A. S. Barker, Jr. (private communication).]
[11] M. Hass, Phys. Rev. Letters **13**, 429 (1964).
[12] M. Hass and H. B. Rosenstock, Phys. Rev. **153**, 962 (1967).
[13] Ronald Fuchs and K. L. Kleiwer, J. Opt. Soc. Am. **58**, 319 (1968).
[14] See, e.g., J. Joos, *Theoretical Physics* (Hafner Publishing Co., New York, 1950), 2nd ed., Chap. 12.

assertion. The surface divergence σ, or surface charge, induced on any ring about the axis of revolution by a field parallel to the surface is proportional to $\cos\varphi$, where φ is the azimuth measured from the direction of the field. (See Fig. 1.) If this assertion is not obvious, it is not hard to prove. (See Ref. 1.) (If we were working with obliquely incident radiation, we would have to consider also a field component of the far field normal to the surface, which would induce a constant σ, rather than a $\cos\varphi$-dependent σ, about any such ring.)

For simplicity, we will use the Gaussian system of units and assume that the medium is in vacuum. We break the surface of a pit or bump into a number of narrow collars. We approximate the exact distribution of surface divergence by assigning to each collar a surface divergence $\sigma_{0j} = \sigma_j \cos\varphi$ over its whole width. Then, we adjust the values of σ_j by solving a set of simultaneous equations so that the electric fields, $\mathbf{E}_1$ and $\mathbf{E}_2$ adjacent to the surface outside and inside the medium, respectively, at the center of each collar satisfy the usual electrostatic-boundary conditions: $\mathbf{E}_1 \times \mathbf{n} = \mathbf{E}_2 \times \mathbf{n}$ and $\mathbf{E}_1 \cdot \mathbf{n} = \epsilon\mathbf{E}_2 \cdot \mathbf{n}$, where $\mathbf{n}$ is a unit vector pointing away from the medium. The first of these conditions will be satisfied implicitly by the method used and only the second appears explicitly in the equations. Since we already know the azimuthal form of the solution ($\cos\varphi$), we only need to match the boundary conditions along a single line of points from the center of the pit out to infinity, or, actually, only to a rather small distance beyond the pit.

By a method described in more detail in the Appendix, we come up with a set of simultaneous equations that have the form

$$\sum_j A_{ij}\sigma_j + \frac{1}{2}\left(\frac{1+\epsilon}{1-\epsilon}\right)\sigma_i = -\mathbf{E}_0 \cdot \mathbf{n}_i. \tag{2}$$

In Eq. (2), $\mathbf{n}_i$ is the surface normal at azimuth $\varphi=0$ in the center of collar i. (See Fig. 1.) $\mathbf{E}_0$ is the electric field that would be just above the surface if the pits were not there. It is the sum of fields from incident and unperturbed reflected radiation. The indices i and j each range from one to the number of collars chosen. A_{ij} represents the normal component of the electric field at azimuth $\varphi=0$ in the center of collar i that would be caused by the surface divergence on collar j alone, if collar j had unit surface divergence at $\varphi=0$.

The matrix A of elements A_{ij} depends only on the shape of the surface and on the somewhat arbitrary choice of collar boundaries. We find that A, and hence σ_j, does not depend on the size of a pit or bump. All geometrically similar surface imperfections yield the same matrix A and the same values of σ_j at corresponding locations. The terms A_{ii}, with like subscripts, represent the normal component of electric field at azimuth $\varphi=0$ in the center of collar i that would be caused by unit surface divergence everywhere on collar i except at that one point. The only term that involves
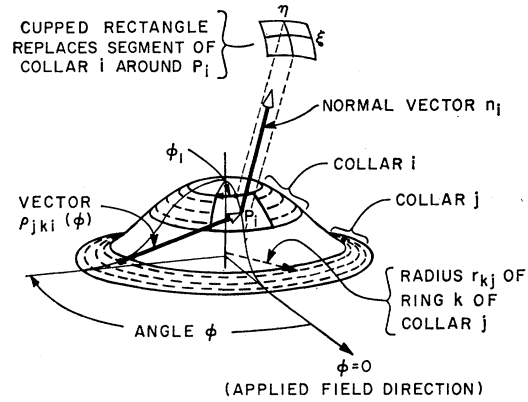

FIG. 1. Variables used in the text. The width of the collars shown is exaggerated. The number of rings (dashed lines) per collar shown is 3, while 5 were used in the calculations.

ϵ is the second term on the left side of Eq. (2), which represents the difference in field across the surface of the medium right at the point P_i at $\varphi=0$ in the center of collar i. (See Fig. 1.)

Having found the values of surface divergence σ_j, it is easy to compute the approximate total horizontal dipole moment P_H for a pit or bump caused by induced surface divergence on and near the irregularity, as seen from the space above it when there is unit field elsewhere just above the surface, parallel to the surface,

$$4\pi P_H = \sum_j \sigma_j \int_0^{2\pi} w_j r_j^2 \cos^2\varphi \, d\varphi = \pi \sum_j \sigma_j w_j r_j^2, \tag{3}$$

where w_j is the width of the collar indexed j, and r_j is the collar radius at its center, so that the area of the collar is $2\pi r_j w_j$. Notice that total polarization is proportional to the cube of any dimension of the pit, and hence is proportional to its volume.

If the normally incident beam of radiation had an electric field of unit amplitude, the electric field amplitude in the beam reflected by a perfectly smooth surface would be

$$R_0 = (1 - \sqrt{\epsilon})/(1 + \sqrt{\epsilon}), \tag{4}$$

where the square root with positive real part is chosen. ($\sqrt{\epsilon}$ is the refractive index of the medium relative to air or vacuum.) The electric field adjacent to the surface in this case would be

$$E_0 = 1 + R_0 = 2/(1 + \sqrt{\epsilon}). \tag{5}$$

The scattering by randomly distributed polarizable dipoles of individual polarization ψ and numerical surface density N (per unit area), located in air above a dielectric surface will modify the reflected beam amplitude, in first-order approximation to

$$R = R_0 + (4\pi^2 i/\lambda)E_0 N\psi(1 + R_0)$$
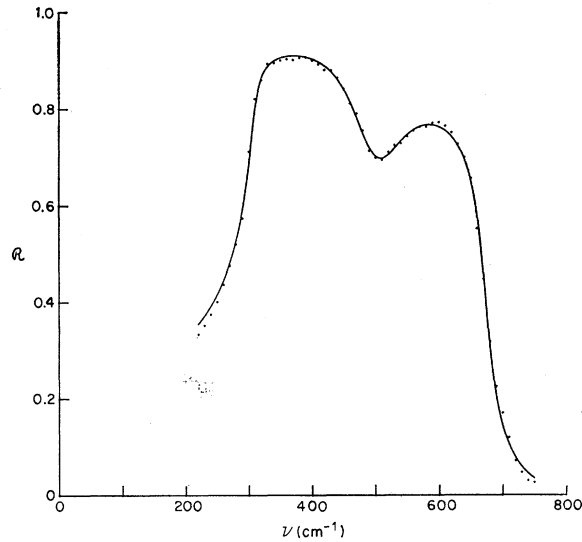$$= R_0\{1 + (16\pi^2 N/\lambda)[i\psi/(1 - \epsilon)]\}, \tag{6}$$

FIG. 2. Reflectance of smooth LiF in the reststrahlen band as a function of incident photon wave number in cm^{-1}. The solid curve is computed from Eq. (10). The dots are data from Jasperse *et al.*

where λ is the wavelength of the radiation and i is now the unit imaginary number. The factor $4\pi^2 i/\lambda$ is a phase and normalization factor that can be derived in various ways, such as by the use of the Fresnel-Kirchoff diffraction formula over all the scattering dipoles. (The sign on this factor was wrong in Refs. 1 and 2.) The factor $(1+R_0)$ on the right in Eq. (6) (beside the factor E_0) takes account of the fact that an oscillating dipole above a surface not only radiates backward but also radiates forward and the forward component is reflected back. (See Sec. IV for a simple example.) (This factor is incorrectly omitted in Refs. 1 and 2.) Equation (6) is equivalent to Eq. (16a) of Strachan[6] for normally incident radiation. $N\psi$ is called σ_2 by Strachan. His derivation uses Sommerfeld's rigorous theory of radiation by dipoles near surfaces[7] and is shown to be valid even if the dipole is moved right down to the surface, a fact that is not obvious from our heuristic argument. A dipole ψ parallel to and just above a dielectric surface casts an electrostatic image in the surface[15] which also has a dipole moment so that the total dipole moment P seen from above the surface (in air) is

$$P = 2\psi/(1+\epsilon). \qquad (7)$$

(We failed to distinguish between P and ψ in Refs. 1 and 2.) Since the imperfections we are discussing are assumed to be so small that the electrostatic approximation is valid locally, we obtain the total dipole moment P as seen from above, when we solve Eq. (3). We may substitute Eq. (7) into Eq. (6), using P obtained from Eq. (3), in order to obtain the first-order

[15] See, e.g., W. R. Smythe, *Static and Dynamic Electricity* (McGraw-Hill Book Co., New York, 1950), 2nd ed., Sec. 5.05, Eq. 3.

correction to the amplitude of a reflected wave. Expanding the square of the absolute value of R from Eq. (6) in powers of NP/λ, we arrive at the following first-order expression for the reflectance of radiation at normal incidence:

$$\mathcal{R} = RR^* = R_0R_0^* \left[1 - \frac{16\pi^2 N}{\lambda} \operatorname{Im}\left(\frac{P(1+\epsilon)}{1-\epsilon} \right) \right]$$

$$= \mathcal{R}_0 + \frac{N}{\lambda}\left[16\pi^2 \mathcal{R}_0 \operatorname{Im}\left(\frac{P(\epsilon+1)}{\epsilon-1} \right) \right], \qquad (8)$$

where $\mathcal{R}_0 = R_0R_0^*$ is the reflectance of a plane surface. Comparison of Eq. (8) with Eq. (1) reveals that

$$\delta = 4\pi\mathcal{R}_0 \operatorname{Im}\left(\frac{4\pi P(\epsilon+1)}{V(\epsilon-1)} \right) = 4\pi\mathcal{R}_0 \operatorname{Im}\left(\frac{8\pi\psi}{V(\epsilon-1)} \right). \qquad (9)$$

IV. SIMPLE EXAMPLES

An unrealistic but easy example of a surface imperfection for which we may obtain an approximate analytic solution may help to clarify the method used here. Suppose the surface had spheres on tall thin stems, like unopened toadstools, distributed on it. The tall stems will be assumed to be short compared to the wavelength of incident radiation and so thin that they have negligible influence on the fields. They are there only to hold up the spheres. The applied field in the neighborhood of a sphere is given by Eq. (5). The polarization of an isolated sphere of volume V per unit applied field is given by the expression

$$\psi = [3(\epsilon-1)/4\pi(\epsilon+2)]V.$$

This expression can be obtained using a spherical harmonic expansion in a uniform field and is a standard elementary electrostatics problem.[14] We have verified that numerically equivalent results are obtained by solving the simultaneous equations of Eq. (1) for surface divergence, using a sphere well above a flat surface, except that we also get polarization on the flat surface below it equivalent to the image, so that the value of P differs from ψ as described in Eq. (7). Notice the resonance that occurs at $\epsilon \approx -2$ for the isolated sphere. If the sphere is far enough from the surface that the field near it is not distorted much by its own image in the surface but is near enough that the uniform part of the field around it is essentially in phase with that at the surface, then the amplitude of radiation in the direction of specular reflection is approximately the sum of the amplitude that would be reflected by the flat surface, plus the amplitude coherently backscattered by the spheres, plus the amplitude coherently forward scattered by the spheres and then reflected back. The first term is R_0 in Eq. (6). The sum of the last two terms is given by the remaining term on the right of Eq. (6). For this simple example, Eqs. (7)

and (9) show that

$$\delta = 4\pi \mathfrak{R}_0 \, \mathrm{Im}[6/(\epsilon+2)], \qquad (8')$$

which has a resonance when ϵ is near -2.

If the stems are made shorter, the electric field around the sphere becomes distorted by the induced polarization in the flat surface below. That induced polarization contributes to the scattering and also changes the polarization of the sphere, so that Eq. (8') is no longer accurate and the resonance occurs at somewhat different values of ϵ and may be smeared out over a broader range of values of ϵ. Then we must resort to a more general method such as the one previously described in this paper to compute δ.

(a)

(b)
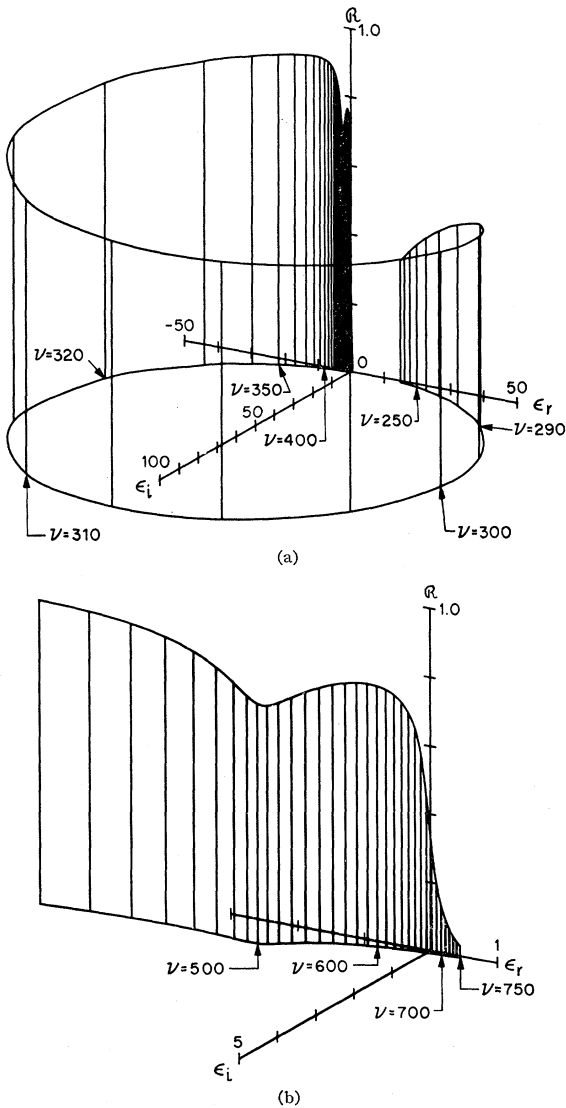
Fig. 3. The same computed reflectance as in Fig. 2 plotted as a function of complex "dielectric constant" ϵ. (a) Shows the whole loop of values through the reststrahlen band. (b) Shows only the portion near $\epsilon = 0$ on an expanded scale.
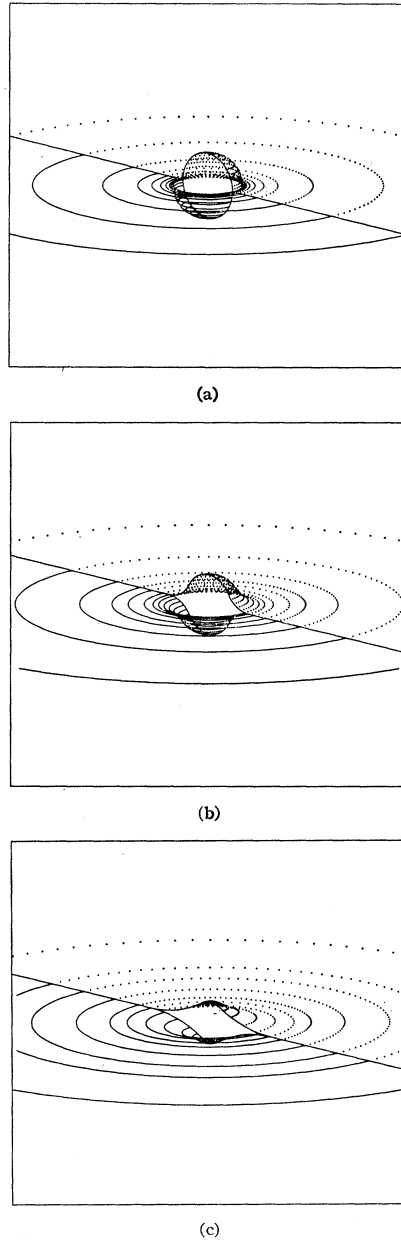

(a)

(b)

(c)

Fig. 4. Half of each type of bump and pit for which computations were made. Solid half-circles are edges of collars used in computations for pits; dotted are those for bumps. (a) Represents hemispheres. (b) Represents figures of revolution with cross section formed by two 60° arcs. (c) Represents figures with two 30° arcs.

Another trivial example that can be solved analytically is that in which the surface imperfection is simply an extremely thin additional flat layer of the same material. For radiation at normal incidence the polarizability ψ/V is just $(\epsilon-1)/4\pi$. Insertion of this value of ψ/V into Eq. (6) gives the phase shift for a surface region differing in height by a very small thickness, $NV \ll \lambda$, from that for which the reflectance amplitude
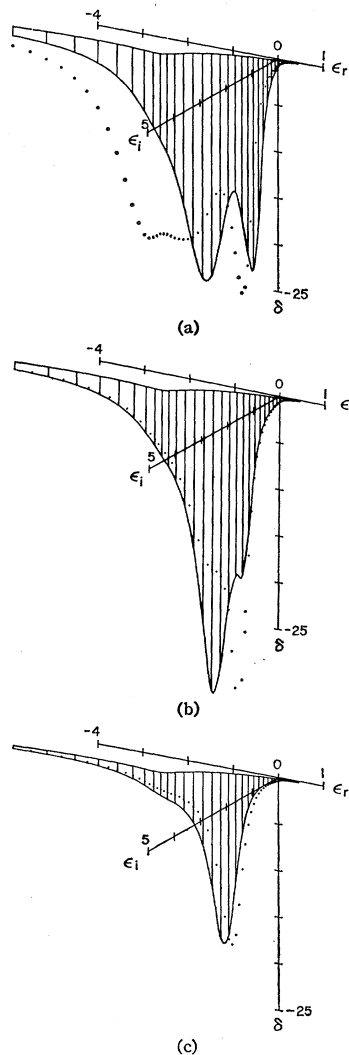
(a)

(b)

(c)

FIG. 5. Correction form factor δ as a function of ϵ along the dispersion curve for LiF in the region near resonance, for each of the irregularities shown in the corresponding parts of Fig. 4. Vertical lines are at ten wave-number intervals where Jasperse et al. measured reflectance. Dotted lines are for bumps, solid for pits. The shallowest pits and bumps have somewhat weaker resonances than the others.

R_0 is computed. For this example there is no change in reflectance. Equation (9) gives zero for δ.

V. NUMERICAL RESULTS

In order to illustrate some practical consequences of the preceding theory, we have computed the reflectance to be expected from slightly roughened lithium fluoride. We refitted room-temperature reflectance measurements, made by Jasperse et al.[16] on carefully polished LiF, with the following dispersion relation for ϵ having two pairs of poles and two pairs of zeros in the complex plane, subject to the condition that the

[16] J. R. Jasperse, A. Kahan, J. N. Plendl, and S. S. Mitra, Phys. Rev. 146, 526 (1966).

sums of the imaginary parts of poles and of zeros are equal[17]:

$$\epsilon = \epsilon_\infty (Z_1 - \nu)(Z_1{}^* + \nu)(Z_2 - \nu)(Z_2{}^* + \nu)/$$
$$(P_1 - \nu)(P_1{}^* + \nu)(P_2 - \nu)(P_2{}^* + \nu). \quad (10)$$

A very good fit was obtained with $\epsilon_\infty = 1.90$, $P_1 = 307.36 - 8.10i$ cm^{-1} $P_2 = 504.50 - 50.86i$ cm^{-1}, $Z_1 = 671.94 - 1198i$ cm^{-1}, and $Z_2 = 491.38 - 47.07i$ cm^{-1}. (The poles and zeros are quite close to the poles and zeros of the classical oscillator dispersion formula fitted to the data by Jasperse et al.) Figure 2 shows the computed and observed reflectance as a function of wave number. Figure 3 shows the computed reflectance of a perfectly flat surface as a function of the complex dielectric constant ϵ computed from the fitted dispersion relation for LiF. Figure 3(a) shows the whole loop of the dispersion curve, while Fig. 3(b) is an enlarged view of the region in which anomalies are expected to occur if the surface is not perfectly flat.

Figures 4(a)–(4c) show the shapes of halves of 3 pits (solid) and 3 bumps (dotted) for which form factors δ
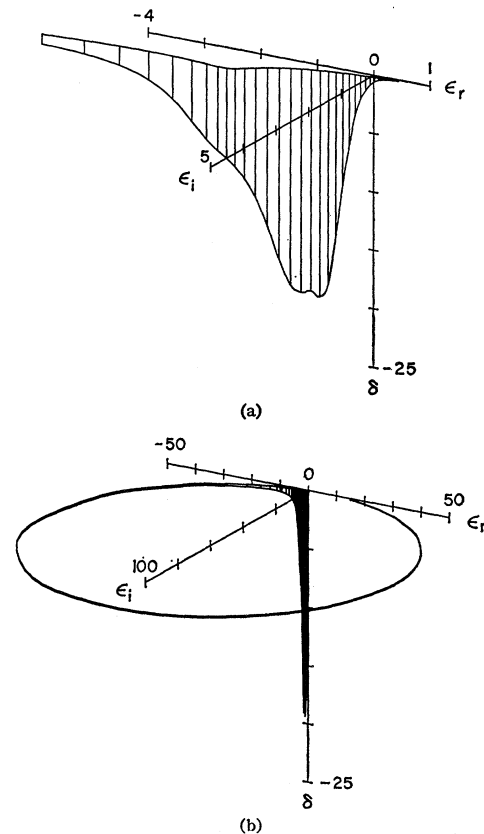

(a)

(b)

FIG. 6 (a) Correction form factor δ for a rough surface having equal numbers of each of the six forms of irregularities, found by averaging the six curves in Fig. 5. (b) Same curve on a reduced scale [cf. Fig. 3(a)] showing whole dispersion loop for LiF and relatively small resonance region.

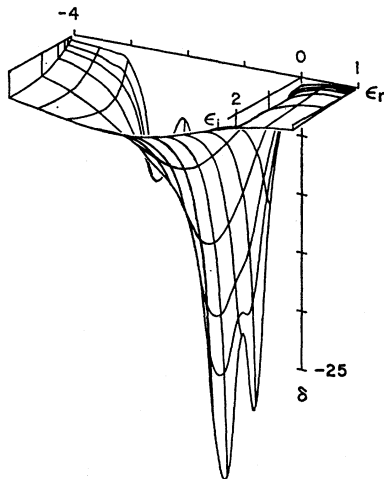[17] D. W. Berreman, Phys. Rev. 174, 791 (1968).

FIG. 7. Correction form factor for the same type of surface roughness described in Fig. 6, plotted along several lines parallel to the real and imaginary ϵ axes to show how localized the resonance effect is in the complex ϵ plane. Contour intersections are at computed points in ϵ, δ space. The curves are interpolated. The "surface" of δ as a function of ϵ can be estimated by interpolation between these curves.

were computed and the edges of each of the "collars" assumed to have approximately radially invariant surface divergence of electric field for each such irregularity. Figures 5(a)–5(c) show the form factor δ of reflectance anomalies for each of the irregularities illustrated in Fig. 4 as a function of ϵ in the region where δ is large [cf. Fig. 2(b)]. Dotted curves are for bumps and solid curves for pits. Vertical bars represent points at which computations were made and at which Jasperse et al. reported measurements of reflectance.

It is interesting to note that there is no great difference between the perturbation caused by a bump and that caused by a pit having the shape of its reflected image, particularly when the bump or pit is rather shallow, as shown in Fig. 5(c). However, there is a tendency for the total strength of the perturbation, represented by the area under the curves, to be somewhat smaller for broad, shallow irregularities than for smaller, deeper ones of the same volume. Thus, a surface with gently rolling contours would not differ as much in reflectance from a flat surface as would one whose irregularities had steeper sides.

Since real rough surfaces are likely to have bumps and pits of various shapes, we took an average of the six form factors illustrated in Fig. 5, which would describe a surface with one-sixth of each of the six types of irregularities, and plotted the form factor for that mixture on Fig. 6(a). Figure 6(b) shows the form factor for the same mixture over the whole infrared dispersion loop for LiF and shows that the form factor is relatively insignificant except in the region of small negative, mostly real values of ϵ.

The dispersion curves of many media, such as ionic semiconductors and many metals, pass through points

much farther from the real axis on the complex ϵ plane than that of LiF even though they may be quite reflective in some regions of the spectrum. Such more optically absorbent media would show much less pronounced perturbation in reflectance caused by surface roughness. Figure 7, which is a three-dimensional plot of the perturbation term δ as a function of both real and imaginary parts of ϵ, illustrates this point. The same mixture of shapes of bumps and pits was used to compute values of δ for Fig. 7 as for Fig. 6. Notice that the decline in absolute value of δ has roughly the same steepness in both real and imaginary directions, as one moves away from the region where ϵ_i is very small and ϵ_r is between about -2 and $-\frac{1}{2}$. In particular, notice how much shallower and smoother the contour is along the line $\epsilon_i = 2$ than along the line $\epsilon_i = 0.1$, the opposite extreme on the graph.

Figure 8 is a plot of the reflectance computed for a LiF sample with the mixture of irregularities just described if the sum of absolute values of volumes of all irregularities per unit area (NV) is equal to 500 Å (dotted line), superimposed on the reflectance curve computed for a perfectly flat sample. 500 Å is a large value for NV compared to the values one might expect for surfaces to be used in optical studies with visible light. However, one might incorrectly suppose that such a surface was good enough for reststrahlen measurements on LiF, where radiation of wavelength 10^5 Å is used. Even a surface with 500 Å root-mean-square (rms) roughness would not look polished (particularly if its visible light scattering were observed in good light), and the parameter NV is generally smaller than the rms roughness.

(As an illustration of the difference between NV and rms roughness, consider a model composed of cubic bumps and pits of side A in a rectangular array
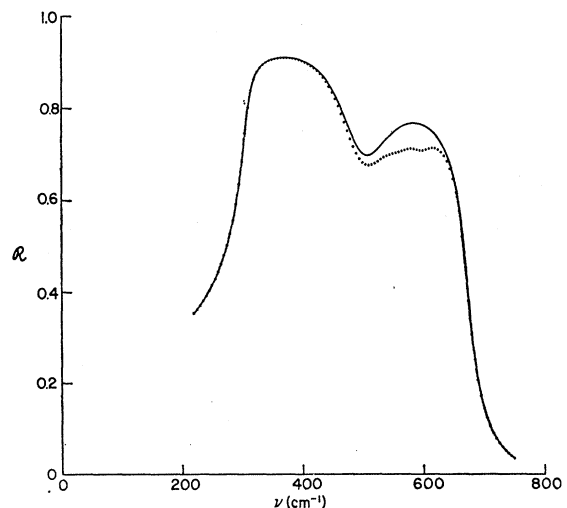

FIG. 8. Reflectance of flat LiF surface (solid line) and reflectance of surface with 500 Å surface roughness of type described under Fig. 6 (dotted line) as a function of wave number.
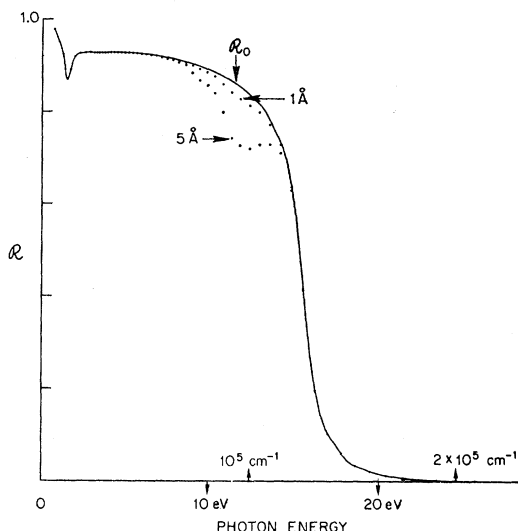
FIG. 9. Reflectance of flat aluminum surface (Ref. 10) (solid line) and reflectance of aluminum with 1 Å and 5 Å roughness parameters (dots) as a function of photon energy.

of spacing $3A$. NV would equal $\frac{1}{9}A$, while the rms roughness parameter would be $\frac{1}{3}A$. The two parameters are not equivalent. The first is the one that is significant for the resonant effects discussed in this paper, while the second is one that is important in the study of incoherent scattering, which is a different phenomenon.)

The reflectance anomaly predicted for LiF by these computations is probably larger than one would actually observe with an ordinary sample with the assumed degree of roughness. This is because samples probably would not have surfaces such that the imaginary part ϵ_i of dielectric constant is as small in the top few hundred Å as it is deeper unless extreme care were taken to relieve strains and avoid other damage that would enhance mode damping near the surface. Larger values of ϵ_i result in weaker resonances, as illustrated in Fig. 7. A layer of material a few hundred Å thick with a value of ϵ_i different from that of the underlying material would not alter reflectance very much unless ϵ_i were small enough for the type of shape-dependent resonance described here to be noticeable, or else were very much larger.

We will not show complete figures for reflectance correction in other types of material. However, we shall briefly describe the effect in aluminum as a second interesting illustration (see Fig. 9). Values of ϵ for aluminum derived from Kramers-Kronig analysis or dispersion curve fitting of reflectance data[10] pass along very nearly the same path at frequencies corresponding to photon energies between about 6 and 16 eV, as those for LiF do between about 400 and 700 wave numbers (cm^{-1}). Hence, the correction form factor δ for any particular surface shape is very nearly the same as for LiF. However, the wavelengths involved [λ in Eq. (1)] are smaller by about two orders of magnitude for alumi-

num than for LiF. Consequently, the measure of roughness that would cause the same change in reflectance for aluminum as was illustrated for LiF is only on the order of atomic dimensions. It is not reasonable to expect accurate results for Al from our method because of our approximation that ϵ is independent of position in the medium. The anomalous skin effect would probably make this a poor approximation. However, our results do indicate that one cannot expect to make an aluminum sample flat enough to obey Fresnel's reflectance equations accurately within that range of photon energies. The difficulty in obtaining reproducible results for reflectance or for ϵ near plasma frequencies in metals is well known and various explanations have been proposed,[18] most of which probably explain parts of the difficulty correctly. In the light of our calculations, the fact that anything near to consistent and reproducible results can be obtained for ϵ at these frequencies seems more surprising than the difficulty in obtaining them.

ACKNOWLEDGMENTS

APPENDIX

We now give a brief exposition of the derivation of Eq. (2), and show the method used to evaluate the matrix elements A_{ij} approximately.

An expression for the local normal component of electric field just outside a point P_i on the surface of a dielectric with electric field surface divergence distribution σ is

$$E_{n+} = \mathbf{E}_0 \cdot \mathbf{n} + \int\int \left(\frac{\sigma \boldsymbol{\varrho} \cdot \mathbf{n}_i d^2\rho}{4\pi\rho^3}\right) + \tfrac{1}{2}\sigma_i. \qquad \text{(A1)}$$

(This equation follows directly from Coulomb's law.) In this equation $\boldsymbol{\varrho}$ is a vector from any point on the surface other than P_i to the point P_i, $d^2\rho$ is an element of surface area, and σ_i is the surface divergence at P_i. (See Fig. 1.) ($\sigma/4\pi$ in Gaussian units, or σ in rationalized units, may be thought of as the charge density on a surface bounded on both sides by vacuum that would produce the same electric fields as the polarized di-

---

[18] See, e.g., *Optical Properties and Electronic Structure of Metals and Alloys*, edited by F. Abeles (North-Holland Publishing Co., Amsterdam, 1966).

electric does.[14]) $\mathbf{n}_i$ is a unit vector normal to the surface at $P_i \cdot \mathbf{E}_0$ is the electric field that exists very near and parallel to the flat surface (for normally incident radiation) far from any imperfection. In this formula we set $\boldsymbol{\varrho} \cdot \mathbf{n}$ equal to 0 near the point P_i. The term $\frac{1}{2}\sigma_i$ may be deleted and taken as part of the double integral if the point at which E_{n+} is measured is taken to be a small but finite distance above the surface.

Just under the surface the normal field component is

$$E_n{}^- = E_n{}^+ - \sigma_i. \tag{A2}$$

The continuity condition for electric displacement normal to a dielectric surface may be written

$$E_n{}^+ = \epsilon E_n{}^-. \tag{A3}$$

Combining the three preceding equations, we obtain

$$\int\int \frac{\sigma \boldsymbol{\varrho} \cdot \mathbf{n}_i}{4\pi\rho^3} d^2\rho + \left(\frac{1+\epsilon}{1-\epsilon}\right)\frac{1}{2}\sigma_i = -\mathbf{E}_0 \cdot \mathbf{n}_i. \tag{A4}$$

We now approximate the double integral by a sum of terms for coaxial collars, each with uniform surface divergence σ_j along the azimuth line at $\varphi = 0$. We see that

$$\int\int \frac{\sigma \boldsymbol{\varrho} \cdot \mathbf{n} d^2\rho}{4\pi\rho^3} \approx \sum_j \sigma_j A_{ij}. \tag{A5}$$

Combining Eqs. (A4) and (A5) leads to Eq. (2). Breaking collars up into K coaxial rings for $j \neq i$, we get

$$A_{ij}(j \neq i) = \frac{w_j}{4\pi K} \sum_{k=1}^{K} r_{jk} \int_0^{2\pi} \frac{\boldsymbol{\varrho}_{jki} \cdot \mathbf{n}_i}{\rho_{jki}{}^3} \cos\varphi \, d\varphi, \tag{A6}$$

where $\boldsymbol{\varrho}_{jki}$ is a vector from a point at φ on the kth ring in the jth collar to a point P_i at the center of the ith collar at $\varphi = 0$, and r_{jk} is the radius of that ring. (See Fig.1 .) The integrals in Eq. (A6) were solved numerically with a computer to obtain matrix elements for bumps or pits of each shape.

To get the term A_{ii} for the collar containing the point P_i, we must cut out a region directly under P_i

and treat it in a more exact manner than using a set of rings as an approximation.

The terms A_{ii} were evaluated by breaking them into two parts, S_i and T_i. S_i is the contribution of the part of collar i that is at angles φ greater than some minimal value φ_1 from the point P_i at $\varphi = 0$. S_i was evaluated numerically in exactly the same way as A_{ij} for $j \neq i$, except that the integral was taken from φ_1 to $2\pi - \varphi_1$, rather than from 0 to 2π [cf. Eq. (A6)]. We chose φ_1 so that the region on the collar contributing the term T_i and omitted from S_i was roughly square. (See Fig. 1.)

In order to evaluate T_i, we replaced the cut-out segment in collar i with a cupped or saddle shaped rectangle having the same two principal values of curvature as the model surface at the point P_i, and having the same width and length as the orthogonal medial lines of the cut-out segment of the collar. Using u and v as the principal values of curvature and ξ and η as the half-width and half-length of the rectangle, we get, by a little geometry and some integral tables,[19] the result that

$$\begin{aligned}
T_i &= \frac{1}{4\pi} \int_{-\xi}^{\xi} \int_{-\eta}^{\eta} \frac{2ux^2 + 2vy^2}{(x^2+y^2)^{3/2}} dx \, dy \\
&= -\frac{2}{\pi} \left(u\eta \log\left\{ \frac{\xi}{\eta} + \left[\left(\frac{\xi}{\eta}\right)^2 + 1 \right]^{1/2} \right\} \right. \\
&\qquad\qquad \left. + v\xi \log\left\{ \frac{\eta}{\xi} + \left[\left(\frac{\eta}{\xi}\right)^2 + 1 \right]^{1/2} \right\} \right). \tag{A7}
\end{aligned}$$

The longest part of the computation is that in which the matrix elements A_{ij} and A_{ii} were evaluated. This was done once for each shape of pit or bump. It is a relatively small job to solve the set of simultaneous equations (2) for various values of ϵ for each shape of irregularity.

---

[19] See, e.g., H. B. Dwight, *Tables of Integrals and Other Mathematical Data* (The Macmillan Co., New York, 1961), 4th ed., Eqs. 200.01, 200.03, 202.03, and 626.2.